Available online at www.sciencedirect.com

ScienceDirect

Energy Procedia 71 (2015) 112 – 122

Energy Procedia

The Fourth International Symposium on Innovative Nuclear Energy Systems, INES-4

Kinetic analysis and prediction of thermal decomposition behavior of tertiary pyridine resin in the nitrate form

Yoshihiko Sato[a]*, Takehiro Matsunaga[b], Shin-ichi Koyama[c], Tatsuya Suzuki[d], and Masaki Ozawa[e]

[a]*Chemical Safety Research Group, National Institute of Occupational Safety and Health, Japan, 1-4-6 Umezono, Kiyose, Tokyo 204-0024, Japan,* [b]*National Institute of Advanced Industrial Science and Technology, 1-1-1 Higashi, Tsukuba, Ibaraki 305-8565, Japan,* [c]*Japan Atomic Energy Agency, 4002 Narita-cho, O-arai, Ibaraki 311-1393, Japan,* [d]*Nagaoka University of Technology, 1603-1 Kamitomioka, Nagaoka, Niigata 940-2188, Japan,* [e]*Tokyo Institute of Technology, 2-12-1 O-okayama, Meguro-ku, Tokyo 152-8550, Japan*

Abstract

The thermal decomposition behavior of the tertiary pyridine resin, which was used during the nuclide-separation process in the Advanced Optimization by Recycling Instructive Elements (Advanced ORIENT) cycle, was investigated in its nitrate form (TPR-NO_3), in order to determine ways of preventing its runaway reaction. A thermal analysis of TPR-NO_3 and an analysis of the gases produced during decomposition were employed for the purpose. In addition, the kinetics parameters were evaluated via a kinetic analysis of the empirical thermal data. Finally, the validity of the reaction model was assessed by comparing the thermal behavior predicted by the estimated reaction model with that determined by the results of a gram-scale heating test performed in our previous study. We found that, when TPR-NO_3 was heated, first, nitric acid was removed. Subsequently, TPR-NO_3 was oxidized by the removed nitric acid. Under the assumption that it took place an autocatalytic oxidation and n^{th} order thermal decomposition in parallel, the thermogravimetric analysis data could be fitted very well using a nonlinear regression model. The thermal behavior of TPR-NO_3 could be predicted by the reaction model determined in this study under conditions where the cooling effect owing to evaporation was ignored. In addition, the maximum temperature and time to maximum rate of a runaway reaction predicted using the determined reaction model gave the result on the side of prudence.

Selection and peer-review under responsibility of the Tokyo Institute of Technology

Keywords: Tertiary pyridine resin; nitrate form; thermal decomposition; kinetics

* Corresponding author. Tel.: +81-42-491-4512; fax: +81-42-491-7846.
E-mail address: sato-yoshihiko@s.jniosh.go.jp

Selection and peer-review under responsibility of the Tokyo Institute of Technology
doi:10.1016/j.egypro.2014.11.861

1. Introduction

The Advanced Optimization by Recycling Instructive Elements (Advanced ORIENT) cycle has been proposed as a part of the efforts to develop new reprocessing techniques for the spent fuel from fast breeder reactors [1]. For separating minor actinides and Sr-Cs during the Advanced ORIENT cycle, we had previously proposed a chromatographic method based on the tertiary pyridine resin (TPR) [2]. The TPR serves two functions: the first is to act as a weak anion exchanger, and the second is to act as a soft donor ligand. Ion-exchange resins have been used for separating nuclides from spent fuel. Nitric acid is also used in the Advanced ORIENT process. However, the use of nitric acid as an eluent has led to explosions in certain cases [3,4]. In response to these explosions, numerous studies have been performed on the reactivity between ion-exchange resins and nitric acid. However, the reaction behavior is still not well understood. Therefore, there is not sufficient information available for designing inherently safe spent fuel-processing techniques. It is possible that TPR may react explosively with nitric acid. However, there have been only a few studies on the thermal decomposition of TPR [5,6]. In addition, the reaction of TPR with nitric acid has not been investigated adequately. In our previous studies on the subject, [7,8] we had attempted to investigate the basic properties of this reaction system in order to determine the thermal stability of the TPR-methanol-hydrochloric acid/nitric acid mixture. It was found that the vigorous exothermic reaction that results could be controlled by manipulating the heating temperature [7].

In this study, the thermal decomposition of TPR in the nitrate form (TPR-NO_3) was evaluated on the basis of simultaneous thermogravimetry-differential thermal analyses and mass spectrometry (TG-DTA/MS) and simultaneous thermogravimetry-differential thermal analyses and Fourier transform infrared spectrometry (TG-DTA/FTIR). In addition, the kinetics parameters of the reaction were determined on the basis of the results of the thermal analyses. Finally, the thermal behavior of TPR-NO_3, determined using the estimated kinetics parameters, was compared with that determined in our previous study using a heating test on the gram scale [7].

2. Experiments

2.1. Samples

TPR, which was a copolymer of vinylpyridine and divinylbenzene, as shown in Figure 1, was synthesized in the laboratory [9]. The particle size of the sample used in the present study was 100–200 mesh, and the degree of cross-linking was 20%. The synthesized TPR sample was conditioned in a solution of hydrochloric acid and then washed with deionized water. 300 mL of a 1 M solution of nitric acid was run through 30 mL of the conditioned TPR sample. Next, 100 mL of deionized water was run continuously through the TPR sample in order to wash it. The presence of chloride ions was tested for by checking whether silver chloride was produced upon the addition of silver nitrate to the nitric acid solution run through the TPR sample. The thus-prepared TPR sample is hereafter referred to as TPR-NO_3. TPR-NO_3 was dried in a vacuum desiccator for over 48 h after the excess water was absorbed by filter paper.

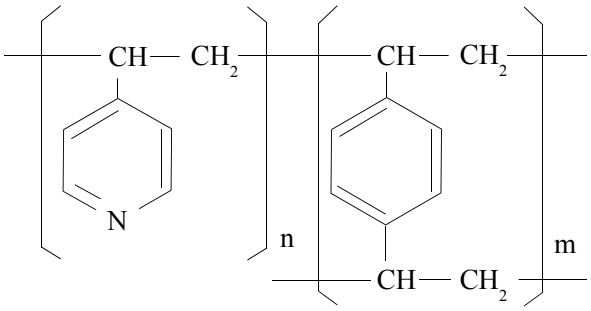

Fig. 1. Chemical structure of TPR.

2.2. Thermal analysis of TPR

The reaction behavior of TPR was analyzed using TG-DTA. TPR was placed in an open aluminum pan and heated from room temperature to 500 °C in a flow of helium; the flow rate was 200 mL min^{-1}. The heating rates employed were 2, 5, 10, and 20 °C min^{-1}.

The reaction products of TPR were analyzed using TG-DTA/MS and TG-DTA/FTIR. TPR-NO_3 was placed in an open aluminum pan and heated from room temperature to 500 °C at a heating rate of 10 °C min^{-1}. In the case of TG-DTA/MS, helium was used at a flow rate of 200 mL min^{-1}. In the case of TG-DTA/FTIR, argon was used at a flow rate of 20 mL min^{-1}. During mass spectrometry, scanning was performed repeatedly, at a rate of 3 s $scan^{-1}$; the range of masses covered was 10–140 u. The infrared (IR) spectra were acquired over wavelengths of 4000–400 cm^{-1}. The resolution was 8 cm^{-1}. All IR spectra were integrated 15 times.

3. Calculations

The reaction kinetics was analyzed using a multivariate nonlinear approximation, which was performed with the NETZSCH Kinetic Software [10]. The activation energy and pre-exponential factor that were used as the initial values for the multivariate nonlinear approximation were estimated via the Friedman method [11] using the experimental TG data.

The Friedman equation is as follows:

$$\ln\left(\frac{d\alpha}{dt}\right)_{\alpha=\alpha_j} = \ln A - \frac{E}{RT} + \ln f\left(\alpha_j\right) \tag{1}$$

where $d\alpha/dt$ is the conversion rate, A is the pre-exponential factor, E is the activation energy, R is the gas constant, T is the absolute temperature, and $f(\alpha)$ is the reaction mechanism function. α is the degree of conversion and is defined as follows:

$$\alpha_j = \frac{m\left(t_s\right) - m\left(t_j\right)}{m\left(t_s\right) - m\left(t_f\right)} \tag{2}$$

where $m(t_s)$ is the thermogravimetric signal at the start time, t_s; $m(t_j)$ is the thermogravimetric signal at time, t_j; and $m(t_f)$ is the thermogravimetric signal at the end time, t_f.

When $\ln(d\alpha/dt)$ is plotted against the reciprocal of the absolute temperature, T, the slope of the linear function is E/R. Therefore, the activation energy can be estimated from the slope of the linear function. Moreover, when the activation energy is fixed, the pre-exponential factor can be determined from Eq. (1).

The number of reaction steps involved was determined by investigating the change in the activation energy with the degree of conversion. On the basis of the estimated activation energy and the pre-exponential factor, the experimental TG data were fitted to the various reaction paths and mechanism functions using multivariate nonlinear regression. The reaction path and mechanism function that fitted the experimental TG data best were investigated. It was surmised that the independent, competitive, and successive reactions shown in Table 1 were the potential reaction mechanisms.

The thermal behavior of TPR-NO_3 was predicted on the basis of the reaction model determined using the above-described method. The validity of the reaction model was assessed by comparing the thermal behavior predicted on its basis and that determined previously using a heating test on the gram scale [7]. The NETZSCH Thermal Simulations Software [12] was used for the prediction, which was made on the basis of the expansion equation of the Thomas model [13]. The equations for this model and the boundary conditions are shown below.

Table 1. Descriptions of various reactions and their equations.

Type of reaction	f(α)
1st order reaction	$1-\alpha$
2nd order reaction	$(1-\alpha)^2$
nth order reaction	$(1-\alpha)^n$
One-dimensional diffusion	0.5α
Two-dimensional diffusion	$[-\ln(1-\alpha)]^{-1}$
Three-dimensional Jander's diffusion	$1.5(1-\alpha)^{2/3}[1-(1-\alpha)^{1/3}]^{-1}$
Three-dimensional Ginstling-Brounshtein diffusion	$1.5[(1-\alpha)^{-1/3}-1]^{-1}$
Two-dimensional phase boundary reaction	$2(1-\alpha)^{2/3}$
Three-dimensional phase boundary reaction	$3(1-\alpha)^{2/3}$
Autocatalytic reaction, according to Prout-Tompkins equation	$(1-\alpha)\alpha$
ath degree autocatalytic reaction with an nth order reaction Prout-Tompkins equation	$(1-\alpha)^a\alpha^n$
1st order reaction with autocatalysis	$(1-\alpha)(1+k\alpha)$
nth order reaction with autocatalysis	$(1-\alpha)^n(1+k\alpha)$
Two-dimensional nucleation, Avrami-Erofeev	$(1-\alpha)[-\ln(1-\alpha)]^{1/2}$
Three-dimensional nucleation, Avrami-Erofeev	$3(1-\alpha)[-\ln(1-\alpha)]^{2/3}$
n-dimensional nucleation, Avrami-Erofeev	$n(1-\alpha)[-\ln(1-\alpha)]^{(n-1)/n}$

$$\lambda\left(\frac{\partial^2 T}{\partial r^2}+\frac{j}{r}\frac{\partial T}{\partial r}\right)+\overline{\rho\cdot c_v}\cdot\frac{\partial T}{\partial t}=\left(-\Delta H\right)\cdot f\left(c,t,T\right) \tag{3}$$

$$-\lambda\left(\frac{\partial T}{\partial r}\right)=k\cdot\left(T_s-T_a\right) \qquad \text{for } r=R_0 \tag{4}$$

$$\frac{\partial T}{\partial r}=0 \qquad \text{for } r=0 \tag{5}$$

where ρ is the density of the reactant, c_v is the specific heat of the reactant, λ is the thermal conductivity of the reactant, r is the radial distance from the center, R_0 is the radius of the cylinder or sphere, $T(r)$ is the temperature at a distance r from the center, T_s is the temperature of the surface of the reactor, T_a is the atmospheric temperature, $-\Delta H$ is the heat of the reaction, j is the shape factor and determined by the shape of the reactor (j = 0: infinite plate, j = 1: infinite cylinder, j = 2: sphere), k is the surface coefficient of heat transfer, $f(c,t,T)$ is a function of the heating rate, c is the concentration of the reactant, t is the time (s), and T is the temperature. The function of the heating rate, $f(c,t,T)$, was used as the mechanism function to determine the best fit to the experimental TG data using multivariate nonlinear regression. The sample geometry and parameters are shown in Fig. 2. The following parameter values were assumed when calculating the thermal behavior: λ = 1.3 W m^{-1} K^{-1}, r = 0.02 m, c_v = 1.34 J g^{-1} K^{-1}, ρ = 1.1 g cm^{-3}, and k = 1.38 W m^{-2} K^{-1}. In addition, an infinite cylinder was assumed. Heat transfer by radiation was ignored. The values of λ, c_v, and ρ stated above were taken from literature [14]. The value of r was obtained from the experimental conditions [7]. The value of k was estimated from the cooling curve of water, which was obtained experimentally [15]. The value of $-\Delta H$ was set to 816 J g^{-1}; this value was taken from previously reported differential scanning calorimetry data [7]. Because it was observed that the methanol coexisting with TPR evaporated, the thermal behavior of TRP after the evaporation of methanol was compared with that predicted by the estimated reaction model.

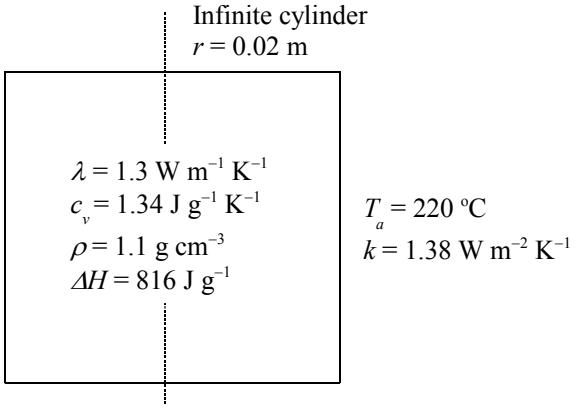

Fig. 2. Sample geometry and parameters used to determine the thermal behavior of TPR-NO_3.

4. Results and discussion

4.1. Investigation of the reaction mechanism of TPR-NO_3

The experimental TG-DTA thermogram of TPR-NO_3 is shown in Figure 3(a). A decrease in weight was observed at 210 °C; the corresponding exothermic peak can be seen in the figure. Moreover, a decrease in weight, which resulted in an endothermic peak, was observed at 370 °C. Further, a slight decrease in weight was observed over the temperature range extending from room temperature to 100 °C. The results of TG-DTA/MS suggested that the primary ions were present in intensity (see Figure 3(b)). At 210 °C, the intensity of the ions with m/z = 18 (H_2O), m/z = 28 (N_2), and m/z = 44 (CO_2 and N_2O) increased, while ions with m/z = 30 (NO) were also observed. Ions with m/z = 39, 51, 63–65, 78, 93, 105, and 119 were observed at 370 °C. It is likely that these ions are the products of the thermal decomposition of TPR. Moreover, the intensity of the ions with m/z = 18 increased with an increase in the temperature from room temperature to 100 °C. Figure 4 shows the IR spectra of the gaseous products at 210 and 370 °C, measured using TG-DTA/FTIR. Absorbance peaks corresponding to CO_2 (asymmetric stretching mode, 2349 cm^{-1}), N_2O (asymmetric stretching mode, 2224 cm^{-1}), and NO (stretching mode, 1875 cm^{-1}) were observed at 210 °C. Absorbance peaks attributable to hydrocarbons and aromatic compounds, in addition to those of CO_2, N_2O, and NO, were observed at 370 °C.

TPR-NO_3 absorbs a small amount of water at room temperature [7]. Thus, the decrease in weight with the increase in the temperature from room temperature to 100 °C can be attributed to the removal of the absorbed water. The exothermic reaction at 210 °C can be explained in terms of the removal of the absorbed nitric acid from TPR-NO_3. Baumann evaluated the thermal stability of a hydroxyl-type quaternary ammonium-type resin [16]. He found that water and methanol were produced by the thermal decomposition of the resin because the OH radicals eliminated from the resin attacked its methyl groups. Given his findings, it is likely that the nitric acid attached to TPR-NO_3 is removed first. Subsequently, water, carbon dioxide, and nitrogen oxides (NO_x) are produced from the oxidation of TPR-NO_3 by the removed nitric acid. The endothermic reaction at 370 °C can be explained in terms of the thermal decomposition of the vinylpyridine-divinylbenzene resin, as is the case with the styrene-divinylbenzene copolymer [17,18]. Styrene and divinylbenzene are produced by the thermal decomposition of this copolymer. Because the chemical structure of the vinylpyridine-divinylbenzene copolymer is similar to that of the styrene-divinylbenzene copolymer, it can be assumed that vinylpyridine and divinylbenzene are produced by the thermal decomposition of the vinylpyridine-divinylbenzene resin.

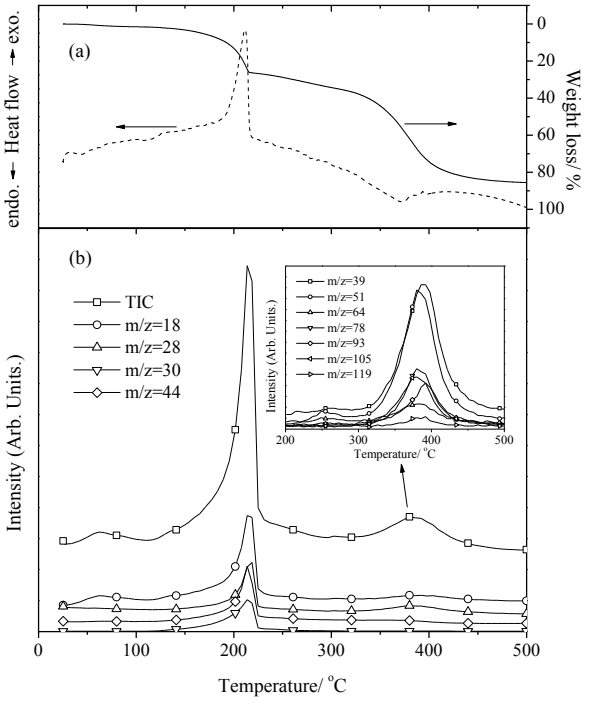

Fig. 3. TG-DTA thermogram and the intensity of the primary ions, determined by the TG-DTA/MS analysis of TPR-NO_3.

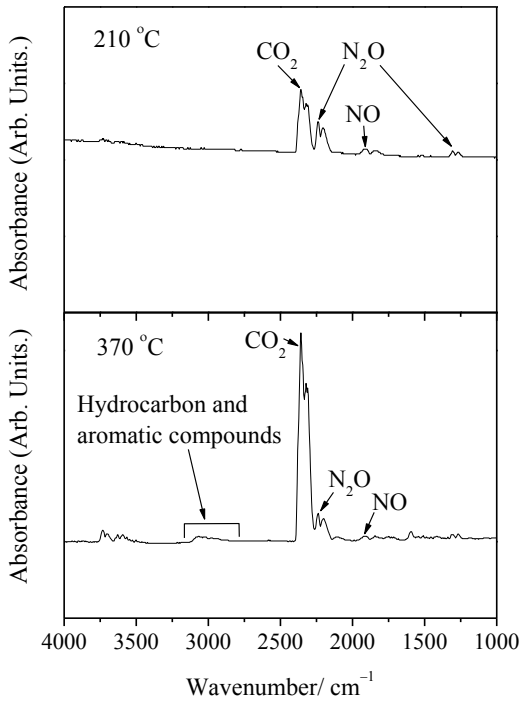

Fig. 4. Infrared spectra of the gaseous products generated at 210 and 370 °C, determined using TG-DTA/FTIR.

4.2. Examination of the kinetics parameters and reaction paths

Figure 5 shows the decrease in the weight of TPR-NO_3 for different heating rates. On the basis of these results, the kinetics parameters and reaction paths of TPR-NO_3 could be determined. The activation energy, E, and pre-exponential factor, A, calculated at each degree of conversion using the Friedman method are shown in Figure 6. The values of E and A corresponding to the different degrees of conversion were different. This means that the decomposition reaction is not a single-step reaction, but a three-step one ($0.1<\alpha<0.3$, $0.3<\alpha<0.6$, and $0.6<\alpha<0.9$). Because the degrees of conversion $0.1<\alpha<0.3$ and $0.6<\alpha<0.9$ correspond to measurement temperatures of 180–215 °C and 370–420 °C, respectively (as determined from the TG data), it would appear that TPR-NO_3 was oxidized by nitric acid at $0.1<\alpha<0.3$, and decomposed thermally at $0.6<\alpha<0.9$. The degree of conversion $0.3<\alpha<0.6$ corresponds to the measurement temperatures of 230–300 °C (also determined from the TG data). Hence, the TG-DTA/MS and TG-DTA/FTIR results were re-evaluated carefully. It was noticed that small amounts of hydrocarbons were produced at 230–300 °C. Therefore, it is postulated that the thermal decomposition of TPR-NO_3 does not occur via a single reaction, but takes place through two consecutive reactions.

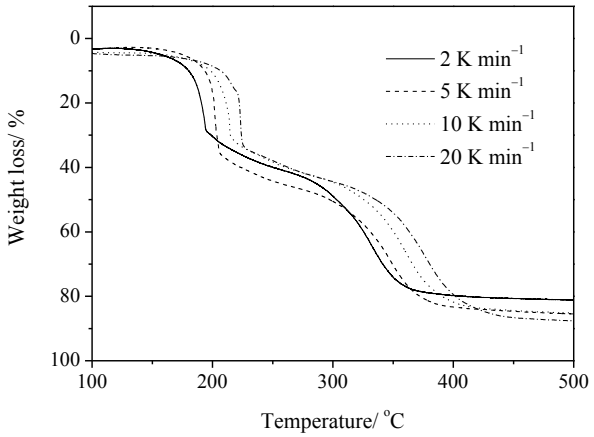

Fig. 5. Loss in the weight of TPR-NO_3 at various heating rates, determined using TG-DTA.

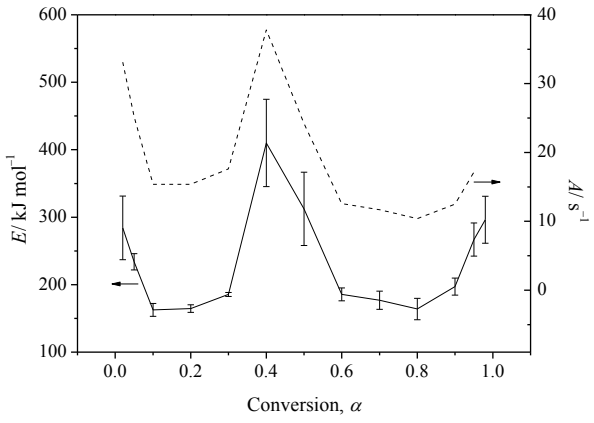

Fig. 6. Values of the activation energy (E) and the pre-exponential factor (A) calculated using the Friedman method.

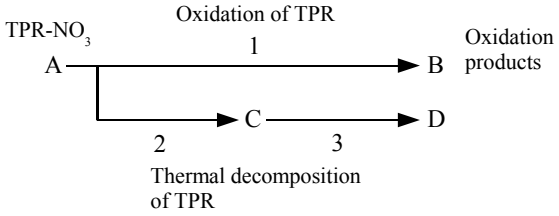

Fig. 7. Possible reaction paths determined on the basis of the results of the thermal and kinetic analyses.

On the basis of these considerations and assuming that the reaction paths are the ones shown in Fig. 7, the kinetic analysis of the TG data of TPR-NO_3 was performed using nonlinear regression. The oxidation of TPR-NO_3 by nitric acid is thought to occur via the reaction path A to B (No. 1). The reaction paths A to C (No. 2) and C to D (No. 3) represent consecutive reactions and are assumed to be the ones responsible for the thermal decomposition of TPR-NO_3, on the basis of the results of the examination of the reaction behavior of TPR-NO_3. Table 1 lists the reaction types used in the kinetic analysis. The best reaction models for reproducing the empirically observed weight loss were determined by applying these reaction types to each reaction.

In the case of the rapid weight loss at approximately 200 °C (path A to B (No. 1)), taking into account the quality of the fit (characterized by the correlation coefficient), it could be seen from Table 1 that the mechanism was similar to that of a Prout-Tompkins type autocatalytic reaction. The oxidation of organic substances by nitric acid proceeds autocatalytically [19,20]. Thus, it is reasonable to approximate the rapid weight loss at approximately 200 °C by the kinetic model of a Prout-Tompkins type autocatalytic reaction. In the case of the weight loss at 230–300 °C (path A to C (No. 2)) and that at 370 °C (path C to D (No. 3)), it could be seen from Table 1 that the mechanism corresponded to that of an n^{th} order reaction. The thermal stability of the styrene-divinylbenzene copolymer has been studied by Gorbachev et al. [18]. They calculated the kinetics parameters on the basis of the mechanism function of an n^{th} order reaction.

Table 2. Kinetics parameters estimated using multivariate nonlinear regression.

Parameter	Optimum value	Standard deviation
ln A_1/ s^{-1}	14.7397	0.2127
E_1/ kJ mol^{-1}	117.5995	0.9679
React. Ord. $_1$	5.5181	0.5045
Exponent a_1	1.3561	0.0720
ln A_2/ s^{-1}	12.0052	0.0642
E_2/ kJ mol^{-1}	114.0888	0.2605
React. Ord. $_2$	5.2540	0.2538
ln A_3/ s^{-1}	11.7725	0.3438
E_3/ kJ mol^{-1}	170.8267	3.8672
React. Ord. $_3$	2.4821	0.0701
CompReact. $_1$	1.1894	0.0648
$CompTotal_{2+3}$	0.8914	0.0234
FollReact. $_2$	0.1895	0.00578
Mass Diff. $_1$/%	–42.4110	Constant
Mass Diff. $_2$/%	–41.3179	Constant
Mass Diff. $_3$/%	–41.8778	Constant
Mass Diff. $_4$/%	–39.6544	Constant

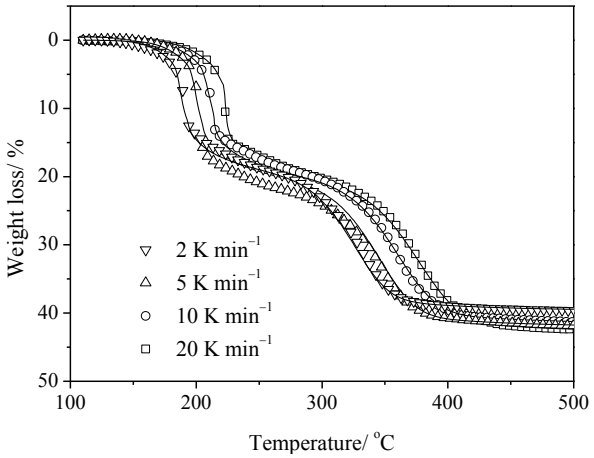

Fig. 8. Loss in the weight of TPR-NO_3 as determined using TG-DTA and the best fits obtained using multivariate nonlinear regression.

Because the chemical structure of the vinylpyridine-divinylbenzene copolymer is similar to that of the styrene-divinylbenzene copolymer, it is reasonable to approximate the weight loss at 230–300 °C as well as that at 370 °C using the kinetics model of an n^{th} order reaction. The curves were obtained by means of nonlinear regression using the above-mentioned mechanism functions (i.e., those corresponding to a Prout-Tompkins-type autocatalytic reaction and an n^{th} order reaction). These curves were fitted to the experimental ones and corrected using the least-squares method. The kinetic parameters after the nonlinear regression are listed in Table 2, and a graphic presentation of the fitted curves is shown in Fig. 8. It could be seen from the figure that the experimental data and the nonlinear regression model fitted extremely well.

4.3. Prediction of the thermal behavior of TPR-NO_3 on the basis of the estimated kinetics parameters

Figure 9 shows the thermal behavior of TPR-NO_3 as predicted on the basis of the estimated reaction model as well as that determined by us previously on the basis of a heating test on the gram scale [7]. In our previous study, we had heated a mixture of TPR, methanol, and nitric acid in a test tube at 220 °C using an adiabatic furnace.

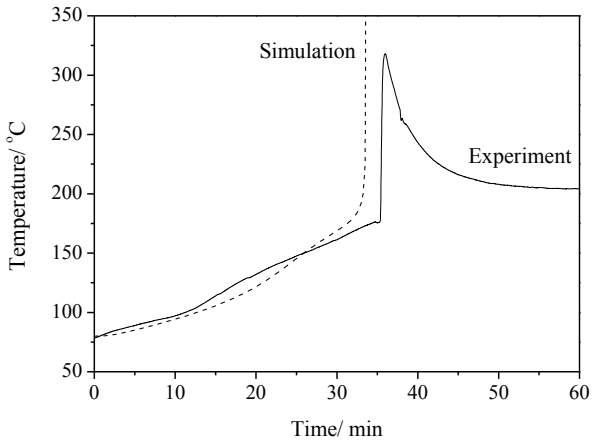

Fig. 9. Comparison of the thermal behavior predicted by the reaction model estimated in the present study and that determined by the results of a heating test on the gram scale.

The temperature of the mixture had been measured with a thermocouple, and the heating process had been recorded with a video camera. The sample temperature had remained at 70 °C, indicating that the methanol had evaporated. At the same time, some of the sample had blown out of the test tube. The sample in the test tube had seemed dry after the evaporation of the methanol. After that, its temperature had been increased slowly to 175 °C and then had increased rapidly. At this point, black fumes had started emanating from the sample. The thermocouple used to measure the temperature of the sample had been placed in it. Because some of the sample had blown out of the test tube, it was likely that the thermocouple had measured the general temperature in the test tube rather than that of the sample. The measured maximum temperature was not the same as that expected, because the temperature within the test tube near the TPR sample was less than what it should have been. However, the experimentally determined time to maximum heating rate was 35 min, while that predicted was 34 min. Thus, the predicted value was almost the same as the experimentally determined one. Furthermore, the maximum temperature and time to maximum rate of the runaway reaction predicted by the estimated reaction model gave the result on the side of prudence. Therefore, it can be surmised that, under conditions where the cooling effect owing to evaporation is ignored, the thermal behavior of TPR-NO_3 can be predicted by the reaction model determined in this study.

5. Conclusions

The thermal decomposition behavior of TPR-NO_3 was estimated on the basis of the results of TG-DTA/MS and TG-DTA/FTIR analyses. In addition, the kinetics parameters of the decomposition reaction were determined from the results of the thermal analyses, and the validity of the reaction model was assessed by comparing the thermal behavior predicted using the model and that determined by the results of a gram-scale heating test that was performed in a previous study. The following conclusions could be drawn:

- The heating of TPR-NO_3 initially resulted in the removal of nitric acid. Subsequently, TPR-NO_3 was oxidized by the removed nitric acid. The thermal decomposition of TPR occurred at a temperature higher than that corresponding to the oxidation.
- Under the assumption that it took place an autocatalytic oxidation and n^{th} order thermal decomposition in parallel, the experimental data obtained from the TG analysis of TPR-NO_3 could be fitted very well using a nonlinear regression model.
- Under conditions where the cooling effect owing to evaporation was ignored, the thermal behavior of TPR-NO_3 could be predicted by the reaction model determined in this study.

References

[1] Ozawa M, Suzuki T, Koyama S, Akatsuka H, Mimura H & Fujii Y. A new back-end cycle strategy for enhancing separation, transmutation and utilization of materials (Adv.-ORIENT cycle). Prog Nucl Energy 2008;50:476-82.
[2] Suzuki T, Fujii Y, Koyama S, Ozawa M. Nuclide separation from spent nuclear fuels by using tertiary pyridine resin. Prog Nucl Energy 2008;50:456-61.
[3] Calmon C. Explosion hazards of using nitric acid in ion-exchange equipment. Chem Eng 1980;87:271-4.
[4] Miles FW. Ion-exchange-resin system failures in processing actinides. Nucl Safety 1968;9:394-406.
[5] Li XG. High-resolution thermogravimetry of poly(4-vinylpyridine-codivinylbenzene). React Funct Polym 1999;42:53-8.
[6] Howell BA, Odelana Adeyinka O. Stability of vinylidene chloride copolymers containing 4-vinylpyridine units: thermogravimetric assessment. J Therm Anal Calorim 2007;89:449-52.
[7] Sato Y, Funakoshi A, Okada K, Akiyoshi M, Matsunaga T, Koyama S, Ozawa M & Suzuki T. Study on thermal stability of tertiary pyridine resin. J Therm Anal Calorim 2009;97:297-302.
[8] Sato Y, Okada K, Akiyoshi M, Matsunaga T, Koyama S, Suzuki T & Ozawa M. Thermochemical safety evaluation of tertiary pyridine resin for the application to multi-functional reprocessing process "Adv.-ORIENT cycle development". Prog Nucl Energy 2011;53:988-93.
[9] Nogami M, Aida M, Fujii Y, Maekawa A, Ohe M, Kawai H & Yoneda M. Ion-exchange selectivity of tertiary pyridine-type anion-exchange resin for treatment of spent nuclear fuels. Nucl Technol 1996;115:293-7.
[10] NETZSCH-Gerätebau GmbH, NETZSCH Kinetic Software, Version 2002.02a.
[11] Freidman HL. Kinetics of thermal degradation of char-forming plastics from thermogravimetry – application to a phenolic plastic. J Polym Sci C 1964;6:183-95.

[12] NETZSCH-Gerätebau GmbH, NETZSCH Thermal Simulations Software, Version 2002.02a.
[13] Thomas PH. On the thermal conduction equation for self-heating materials with surface cooling. Trans Faraday Soc 1958;54:60-5.
[14] Ito K. Plastic Data Handbook. Tokyo: Kogyo Chosakai Publishing Co., Ltd.; 1980 (in Japanese).
[15] Sato Y, Okada K, Akiyoshi M, Matsunaga T, Suzuki T, Koyama S & Ozawa M. The thermal stability of tertiary pyridine resin for the application to multi-functional reprocessing process –Adv.-ORIENT cycle development–. Proc. GLOBAL 2009:962-9.
[16] Baumann EW. Thermal decomposition of Amberlite IRA-400. J Chem Eng Data 1960;5:376-82.
[17] Tou JC. Thermal analysis of the pyrolytic behaviors of a highly crosslinked polymer. J Polym Sci Part A 1984;22:3851-64.
[18] Gorbachev VM, Durasov VB & Gimelsheyn F Ya. Kinetics of thermal destruction of styrene-divinylbenzene copolymers, computed from thermoanalytical data. J Therm Anal 1982;23:167-72.
[19] Hsueh KH, Chen WT, Chu YC, Tsai LC & Shu CM. Thermal reactive hazards of 1,1-bis(*tert*-butylperoxy)cyclohexane with nitric acid contaminants by DSC. J Therm Anal Calorim 2012;109:1253-60.
[20] Holvách M, Lengyel I & Bazsa G. Kinetics and mechanism of autocatalytic oxidation of formaldehyde by nitric acid. Int J Chem Kinet 1988;20:687-97.